Int. J. Heat Mass Transfer. Vol. 16, pp. 3–12. Pergamon Press 1973. Printed in Great Britain

PECULIARITIES OF EVAPORATIVE COOLING IN RAREFIED GAS

A. V. LUIKOV, L. L. VASILIEV and O. G. RASIN

Heat and Mass Transfer Institute, Byelorussian Academy of Sciences, Minsk, U.S.S.R.

(*Received* 14 *January* 1971)

Abstract—The process of evaporative cooling of porous bodies is considered under conditions of rarefaction and simultaneous external and internal heat fluxes.

On the basis of theoretical analysis and experimental study the main relationships are established and optimal conditions are obtained of evaporative cooling. Evaporation mechanism of liquid cooling under vacuum is shown to be controlled by thermophysical and structural properties of the porous body and the recession of the evaporation zone.

NOMENCLATURE

T, temperature;
U, flow velocity;
P, overall pressure of vapour–gas mixture;
P_1, partial vapour pressure;
ρ, density;
q, heat flux;
j, evaporation rate;
α, heat-transfer coefficient;
k, overall heat transfer coefficient;
λ, thermal conductivity;
$\dot{m}$, mass velocity of air flow;
m, mass flow rate of vapour;
D, diffusion coefficient;
η, dynamic viscosity coefficient;
δ, thickness of porous body;
C_p, heat capacity of coolant;
r, latent heat of evaporation;
Λ, mean molecular free path length;
f_n, transverse mass flow factor;
b, pore radius;
ε, phase conversion number;
ξ, recession of evaporation zone;
x, vertical coordinate;
y, horizontal coordinate;
x_0, initial unheated section of porous plate.

Subscripts

∞, flow core;
s, solid surface;
b, solid;
o, normal conditions;
z, evaporation zone.

VERY few experimental data are available on the process of liquid evaporation, although it is a subject of present-day importance in the field of evaporative cooling, intensification of dehydration processes and cryogenic thermostating of superconducting transmission lines.

Necessity of cooling for the purpose of thermal protection or cryogenic thermostating of superconducting transmission lines is commanded by both external and internal (generating within an object) heat fluxes. The latter circumstance makes application of evaporative cooling preferable compared with porous cooling using cold gas blowing. Because of high phase transition heat, evaporative cooling is economic and effective. With evaporation process arranged rationally, it appears possible to achieve a lower surface temperature than the temperature of liquid cooling agent at the inlet, and this not only simplifies the preliminary temperature preparation of the cooling agent but also permits simultaneous heat protection from external loads and a removal of heating power generated within a body to be accomplished.

However, all advantages of evaporative cooling can be realized at full length only under certain optimal conditions, the proper choice of which runs into difficulties due to complicated physical processes accompanying evaporative cooling.

Let us consider evaporative cooling of a porous surface contacted with a heated gas flux. To separate the influence of internal and external conditions adiabatic evaporation regime is assumed when all the heat supplied to the body surface is consumed for phase transition that proceeds over the body surface, the internal heat being equal to zero.

In this case a condition for steady-state evaporation is

$$q_{\text{con}} = q_{\text{evap}}$$

where $q_{\text{con}} = \alpha(t_{\infty} - t_s) = \alpha\Delta t$ is a convective heat flux from the heated gas flow to the body; $q_{\text{evap}} = jr$—is a heat sink due to coolent agent evaporation.

The temperature difference Δt showing a neutralization degree of heat load over the external porous wall surface may serve as a characteristic of evaporative cooling efficiency equal to

$$\Delta t = \frac{jr}{\alpha}. \tag{1}$$

Cooling effect increases with a growth of evaporation rate and a decrease of heat load α. These components are controlled respectively by diffusion and thermal boundary layers. Because of high diffusion resistance of air under conditions of normal density, which results in small Δt, the effectiveness of evaporative cooling under such conditions is low.

Now consider transformation of equation (1). Treating evaporation as a diffusive process, its intensity can be expressed by the Stefan formula as

$$j = -\frac{D}{R_1 T}\frac{P}{P - P_1}\frac{\mathrm{d}P_1}{\mathrm{d}y} = -\frac{D_0}{R_1 T}\frac{760}{P} \times \frac{P}{P - P_1}\frac{\mathrm{d}P_1}{\mathrm{d}y} = -\frac{D_0 760}{R_1 T}\frac{1}{P - P_1} \times \frac{\mathrm{d}P_1}{\mathrm{d}y} = \frac{a}{P - P_1}\frac{\mathrm{d}P_1}{\mathrm{d}y}. \tag{2}$$

For the case of a cooled wall with heated gas in laminar flow the heat-transfer coefficient is

$$\alpha = 0{\cdot}332\,\lambda(^3\sqrt{Pr})\sqrt{(m/\eta x)} = b\sqrt{m}. \tag{3}$$

Substituting j and α from expressions (2) and (3) into (4) yields

$$\Delta t = \frac{r\alpha}{b}\frac{1}{\sqrt{\dot{m}}}\frac{1}{P - P_1}\frac{\mathrm{d}P_1}{\mathrm{d}y}. \tag{4}$$

With constant mass flow rate of air (m = const) the heat-transfer coefficient α and consequently the external heat load, q_{con}, according to equation (3) remain unchanged. However, from the equality $m = U_{\infty}\rho = U_{\infty}P/RT$ it follows that velocity U_{∞} is inversely proportional to P. From experiments on isothermal evaporation of liquids it is known that evaporation rate is proportional to gas rate to the power 0·5 (according to some authors the power on U_{∞} ranges from 0·5 up to 0·8) which, connected with influence of gas flow rate on the partial vapour pressure gradient, yields

$$\frac{\mathrm{d}P_1}{\mathrm{d}y} \propto U^{\frac{1}{2}} \propto \frac{1}{P^{\frac{1}{2}}}. \tag{5}$$

On substitution of (5) into (4)

$$\Delta t \propto \frac{ra}{b\sqrt{m}}\frac{1}{P - P_1}\frac{1}{P^{\frac{1}{2}}}; \qquad \Delta t \propto \frac{c}{P^{\frac{3}{2}}}. \tag{6}$$

Analogous result is obtained if it is assumed that U_{∞} = const. In this case expression (3), since $(\sqrt{m}) = \sqrt{(U_{\infty}P/\dot{R}T)} \propto \sqrt{P}$, may be transformed in the following manner

$$\alpha = b(\sqrt{m}) \propto b\sqrt{P}.$$

Then

$$\Delta t = \frac{rj}{\alpha} \propto ra \frac{\mathrm{d}P_1}{\mathrm{d}y} \frac{1}{P - P_1} \frac{1}{bp^{\frac{1}{2}}} \propto \frac{ra}{b} \frac{\mathrm{d}P_1}{\mathrm{d}y}$$

$$\times \frac{1}{P - P_1} \frac{1}{P^{\frac{1}{2}}}; \qquad \Delta t \propto \frac{c}{p^{\frac{3}{2}}}.$$

Thus, from the point of view of its efficiency, evaporative cooling is advantageous under vacuum conditions. A pressure exceeding slightly that of saturated vapour at evaporation temperature should be taken as the lower rarefaction limit; boiling, which occurs at lower pressure leads to unproductive coolant flow rate because of entrainment of liquid droplets thrown out of the boundary layer. Pressure at the triple point may serve as an orientation mark.

Analysing evaporative cooling it should be kept in mind that the heat-transfer coefficient α depends not only on external thermo- and hydrodynamic conditions over the body surface but also on the evaporation process itself.

The influence of the transverse evaporated mass flow on the heat-transfer coefficient is complex. In experiments on liquid evaporation from an open surface or from porous bodies with convective heat supply there is found both an increase and decrease in the heat-transfer coefficient as compared with that for pure heat transfer. Analytical solution of differential transport equations for porous blowing of gases into the laminar boundary layer, carried out by Eckert and Hartnett [1], predicts a decrease of the heat-transfer coefficient with an increase of the transverse mass flow, expressed by the transverse flow factor $f_n = w_n/w_x \sqrt{Re_x}$. At $f_n = 0{\cdot}05$ the heat-transfer coefficient decreases by 10 per cent and, at $f_n = 0{\cdot}64$, $\alpha \to 0$. For the case of evaporation, as is shown in [2], the transverse flow factor is extremely small and under adiabatic conditions it may achieve 0·05 only at the temperature difference $\Delta t = 260°\mathrm{C}$. At moderate heat loads low-intensity evaporation causes an increase of the heat-transfer coefficient that may be explained by the disturbing effect of a small transverse flow on the boundary-layer structure and also by volume evaporation of liquid droplets. An intensifying influence of small transverse flows on heat transfer is also evident in experiments with weak blowing of gases.

In general, it may be concluded that because of low evaporation rate and intensifying influence of the transverse vapour flow on heat transfer the adiabatic evaporative cooling at normal density of the surrounding medium proceeds under unfavourable conditions.

Evaporative cooling advantages are more fully utilised if the process proceeds in a non-adiabatic regime and under rarefaction conditions. The non-adiabatic regime may be achieved by liquid evaporation within the capillary-porous body and also by carrying out not only convective but conductive heat supply as well. Such a scheme of the evaporation process is of particular practical interest since it corresponds to a real case of evaporative cooling application under the conditions of combined external and internal loads. With a presence of a dry body region between the outer surface and evaporation zone an interconnection of transfer processes in the boundary layer with evaporation process is not limited now by the transverse flow effect on the heat-transfer coefficient but also comprises an influence of thermophysical and structure-porous characteristics of a capillary-porous body. In this case heat transfer between the evaporation surface and surrounding medium proceeds as heat transmission and is

but by the overall heat-transfer coefficient k, equal to

$$\frac{1}{k} = \frac{1}{\alpha} + \frac{\xi}{\lambda_b}. \tag{7}$$

Convective heat transfer of a moist capillary-porous body heated by a gas flow is analysed theoretically in [3] with special regard for the recession of the evaporation zone. It was found that the heat-transfer coefficient depends not only on flow hydrodynamics (the number Re) and its properties (the number Pr) but on position of evaporation zone ξ and thermophysical body properties λ_b as well.

Having solved the differential heat-transfer equation by the Krischer method, the analytical expression is obtained as

$$Nu_x = \frac{1}{\sqrt{\pi}} \sqrt{(Pe_x)}\, N(K, B) \tag{8}$$

where $K = \lambda_b x/\lambda\xi Pe_x^{-0\cdot 5}$ is a recession parameter of the evaporation surface; N is a dimensionless gas flow (blowing) parameter and $N(K, B)$ is a function.

In the case under consideration convective heat transfer should be described by the criterial relationship of the type

$$Nu_x = f(Re_x, Pr, N). \tag{9}$$

From the predicted relationships it follows that with recession of the evaporation surface the heat-transfer coefficient increases.

With an increase of thermal conductivity coefficient λ_b of the solid body the heat-transfer coefficient decreases.

Thermal resistance value of the dry body region defined by the second term of expression (7) is proportional to depth of the evaporation zone and inversely proportional to thermal conductivity coefficient λ_b of the solid body.

Therefore, a change of ξ and λ_b leads to opposite results, for instance, increase in ξ and decrease in λ_b cause simultaneously an increase of the heat-transfer coefficient and an increase of the thermal wall resistance.

The appearance of a dry porous material interlayer between the evaporation surface and the external medium exerts a considerable influence on the mass-transfer mechanism. According to the Stefan law

$$j = -\frac{D}{RT}\frac{P}{P - P_1}\frac{dP_1}{dy} \tag{10}$$

vapour is transferred by a diffusive-convective way. With liquid evaporation from the body depth there takes place a diffusive penetration of a non-condensing gas into a porous body that promotes formation of two-phase flows and appearance of an overall pressure gradient. It is established in reference [4] that for the viscous regime of vapour–gas mixture flow through pores of radius b the overall pressure drop in the body is defined by the expression

$$\frac{(P_z + P_s)(P_z - P_s)}{16MRT\rho D} = \frac{1}{b^2} \ln \frac{1 - P_{1z}/P_s}{1 - P_{1z}/P_z}. \tag{11}$$

From relation (11) it follows that in the vicinity of the triple point (i.e. at $P_{1z} \to P_z$) the overall pressure drop in the porous body may achieve a considerable value.

To check up evaporative cooling relationships considered above and to establish peculiarities occurring in the process mechanism under the influence of rarefaction and internal heat flux,

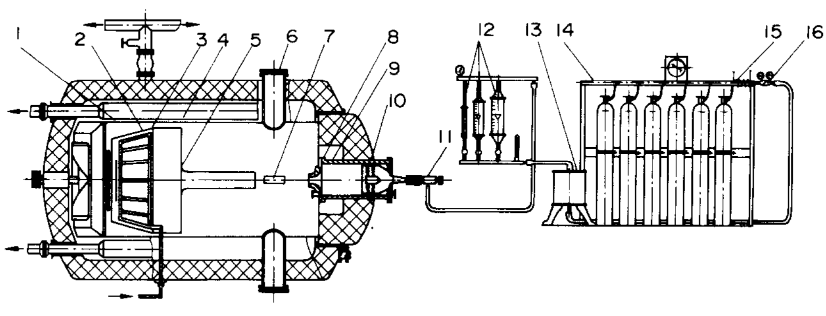

FIG. 1. Experimental vacuum installation. 1, internal wall of thermal vacuum chamber; 2, screen; 3, cryogenic condensation counter; 4, Freon evaporators; 5, diffuser; 6, optical illuminators; 7, working plate; 8, subsonic nozzle; 9, surge vessel; 10, electric heater; 11, vacuum leak valve; 12, flow meter group; 13, drying agent of gas; 14, bulb ramp; 15, thermostabilizing heater; 16, gas reducing valves.

an experimental study was carried out on evaporation process of a liquid from a capillary-porous body into a rarefied gas flow with internal and external heat loads simultaneously affecting the body.

Experiments were run on a special vacuum gas-dynamic installation (Fig. 1) which allowed a change in gas flow parameters in the ranges: temperature $T_\infty = 300$–400 K; static pressure $P_\infty = 10^2$–10^5 N/m^2; flow velocity $u_\infty = 3$–10 m/s. The desired rarefaction in the vacuum chamber was maintained by mechanical pumps. The gas-dynamic installation consisted of a subsonic nozzle 140 mm dia., a surge cylinder with an electrical gas heater, a vacuum micrometric leak valve, gas flow meters and a gas dehydration system. A cryogenic condensing arrangement cooled by liquid nitrogen was set along the chamber axis. When using easily condensing gases cryogenic evacuation permitted to conduct experiments with mechanical pumps switched off.

As a porous body a use was made of beds of spheres placed into the experimental volume with powder-vacuum heat insulation. A spiral heat exchanger was fitted below the body.

A temperature field in the porous body was measured in three sections by a set of differential copper–constantan thermocouples, connected to a multiple-point electronic potentiometer circuit: control measurements were made with a high-precision low-ohmic potentiometer. Temperature distribution in the boundary layer was measured with three microthermocouples located on a special coordinate table, microthermocouples coordinates being defined by means of a cathetometer.

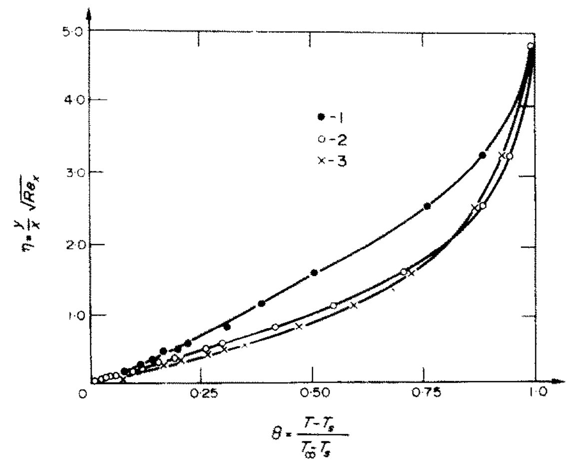

FIG. 2. Temperature distribution in the boundary layer with liquid evaporation from porous nickel. 1, plate centre: 2, beginning of plate; 3, "dry" heat transfer.

Liquid supply to the lower porous body surface was brought about with the help of a special vacuum manostat; into the evaporative zone the liquid was supplied by means of capillary pressure. Mass flow rate was determined by the volume method.

Heat-transfer coefficient was calculated on the basis of temperature field measurements in the boundary layer

$$q_x = \lambda \frac{\partial t}{\partial y_{y=\delta}}; \qquad \alpha = \frac{q_x}{T_\infty - T_s} = \frac{\lambda}{T_\infty - T_s} \frac{\partial t}{\partial y_{y=\delta}}. \tag{12}$$

Liquid evaporated from porous materials with different thermal conductivity. Figure 2 presents curves of the dimensionless temperature distribution $\theta = [(T - T_s)/(T_\infty - T_s)]$ as a function of the generalized coordinate $\eta = (y/x)\sqrt{(Re_x)}$ for the case of distilled water evaporated from a bed of nickel spheres 0·2 mm dia. at the following air flow characteristics: $P_\infty = 33{\cdot}3 \,.\, 10^2$ N/m^2; $T_\infty = 70°$C; $V_\infty = 3$ m/s (mass flow velocity $m = 100$ g/m^{2}s). Evaporation rate was 0·5 g/m^{2}s. Measurements were made in three sections of a boundary layer: over the porous body centre, in an initial body section and over an impermeable leading edge. It is seen that the profile for a "pure" heat transfer is steeper than that for heat transfer complicated by mass transfer; relation α/α_0 appears to be equal to $\backsim 0{\cdot}65$. This is in a good agreement with theoretical predictions [1] in accordance with which for the transverse flow factor f_n being equal in our case to 0·17 the relation $\alpha/\alpha_0 = 0{\cdot}68$.

Temperature distribution within the porous wall is shown in Fig. 3. For a comparison of efficiency of different cooling methods in addition to experimental data in the chart there are presented temperature curves calculated for circulating cooling, porous gas blowing and

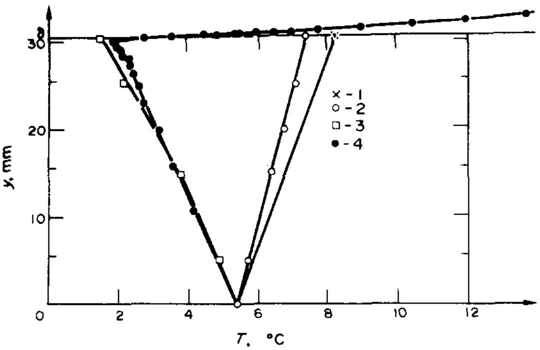

FIG. 3. Temperature within porous nickel.
1, circulating cooling
2, cold air blowing
3, evaporation from body surface } predicted data
4, evaporation from porous nickel

evaporative cooling of liquids over the body surface according to the following equations

$$t = t_0 + y\,\frac{t_s - t_0}{\delta};$$

$$t_s = \frac{t_0 + (\alpha_0 \delta t_\infty / \lambda_{ef})}{1 + (\alpha_0 \delta / \lambda_{ef})} = 8{\cdot}5\,°C \qquad (13)$$

$$t = t_0 + \frac{t_s - t_0}{e^{\xi\delta} - 1}(e^{\xi y} - 1);$$

$$t_s = \frac{t_0\,e^{\xi\delta} + (\alpha/c_p m)\,t_\infty(e^{\xi\delta} - 1)}{e^{\xi\delta} + (\alpha/c_p m)(e^{\xi\delta} - 1)} = 7{\cdot}5\,°C \qquad (14)$$

$$t = t_0 + \frac{mr - \alpha(t_\infty - t_0)}{\alpha - (\alpha - mc_p)\,e^{\xi\delta}}(e^{\xi y} - 1);$$

$$t_s = \frac{\alpha t_\infty(e^{\xi\delta} - 1) + c_p m t_0\,e^{\xi\delta} - mr(e^{\xi\delta} - 1)}{\alpha(e^{\xi\delta} - 1) + c_p m\,e^{\xi\delta}} = 1{\cdot}5\,°C. \qquad (15)$$

Equations (14) and (15) are differential heat-transfer equation solutions of the type

$$\frac{d^2 t}{dy^2} - \xi\frac{dt}{dy} = 0; \qquad \xi = \frac{c_p m}{\lambda_{ef}}; \qquad (16)$$

with the third-kind boundary conditions which for gas blowing and liquid evaporation over the body surface are of the form

$$y = 0 \qquad t = t_0$$
$$y = \delta \qquad \alpha(t_\infty - t_s) = -\lambda_{ef}\frac{dt}{dy} \qquad (17)$$

and

$$y = 0 \qquad t = t_0$$
$$y = \delta \qquad \alpha(t_\infty - t_0) - \lambda_{ef}\frac{dt}{dy} = rj. \qquad (18)$$

Heat-transfer coefficients were determined from the equation

$$\alpha = 0{\cdot}332\,\lambda\,Pr^{\frac{1}{3}}\sqrt{(U_\infty/\nu x)}/{}^3\sqrt{[1 - (x_0/x)^{\frac{3}{4}}]} \qquad (19)$$

and corrected for transverse flow by the transverse flow factor f_n.

Calculations were done from the constancy condition of the inner wall surface temperature ($t_0 = 5{\cdot}5$°C) and the same value of coolant flow rate for cooling by means of mass transfer ($m = 0{\cdot}5$ g/m^{2}s). Calculational results verified the considerations above on advantages of evaporative cooling. These advantages are not limited to the considerably lower surface temperature (1·5°C for evaporative cooling compared with 7·5°C and 8·5°C for gas blowing and circulating cooling, respectively). Problems appear to be quite different for the condition t_0 = const. to be satisfied. If, with circulating porous cooling, a heat flux equal respectively to $q = 84$ W/m^2 and $q = 56$ W/m^2 is directed into an object, then with evaporative cooling one may succeed in removing a heat flux 15–20 times greater ($q = 1170$ W/m^2) from the object.

The experimental temperature profile in a nickel bed somehow differs from that for the case of liquid evaporation over a body surface. There are three characteristic sections standing out in the curve. Temperature drop in the lower section, occupying the basic part of the curve, is of almost linear character. A body in this zone is fully saturated with liquid, heat is mainly transferred by heat conduction.

In the middle part the temperature drop proceeds with an increasing rate. Such temperature distribution is connected with liquid evaporation over the zone volume. The phase transformation criterion ε is a coordinate function and changes within $0 < \varepsilon < 1$. As a result, the body moisture content decreases with height and this leads to a sharp decrease of the effective thermal conductivity coefficient along the zone height. The minimum temperature within a body is observed at the boundary between the middle and upper sections of the curve.

The upper section of the curve characterizes the process in a comparatively narrow surface zone of a body. Owing to decrease in moisture content the evaporation rate falls and, on approaching the surface, it compensates less and less the external heat flux which leads to the gradual body heating in the surface zone.

A sufficiently close coincidence of the experimental minimum temperature values fixed in the body (1·8°C) and the surface temperature predicted by equation (15) ($t_s = 1{\cdot}5$°C) testifies that all the supplied liquid coolant is consumed for evaporation. Calculation of the heat balance equation also indicates that liquid fully evaporates within a porous body, molar carry-over of liquid droplets into the surrounding medium does not practically exist.

Evaporation from the nickel bed, corresponding to evaporative cooling for the case of a body with high thermal conductivity, proceeded at small lowering of the evaporation zone and was characterized by a removal of the large internal heat flux with a rather economical coolant flow rate. This allows to treat high thermal conductivity of a porous body material and small recession of evaporation surface as optimum conditions for evaporative cooling of objects with a considerable inner heat release. However, if a problem of evaporative cooling lies in protection from the external heat load, such a system appears to be unsuitable since it creates favourable conditions for the external heat flux penetration into a body. In this case an application of materials, which are poor heat conductors, appears to be most satisfactory. However, rational utilization of such materials represents a comparatively complex problem because of the evaporation peculiarities experimentally found in materials with a low thermal conductivity.

As a porous body with low thermal conductivity a bed of glass spheres 0·2 mm dia. was used. An effective thermal conductivity of such a bed is; for dry state 0·147 W/m^2°C, for water saturation state 0·84 W/m^2°C. With water evaporation rate equal to 0·3 g/m^{2}s the external surface temperature was 8°C, the minimum temperature in the body 1°C, and the internal surface temperature 9°C. Calculation of the surface temperature by equation (15) with the reference data $j = 0{\cdot}3$ g/m^{2}s, $t_0 = 9$°C gave $t_s = -13{\cdot}3$°C. Therefore, a considerable part of liquid coolant was not involved in the evaporation process. It follows from the heat balance equation that surface cooling up to 1°C (i.e. the minimum temperature fixed in the body) demands an evaporation rate equal to 0·1 g/m^{2}s. While measuring temperature in the boundary layer, in the presence of such an intensive molar liquid removal, there was observed a stepwise temperature change in the vicinity of the surface of the body (Fig. 4).

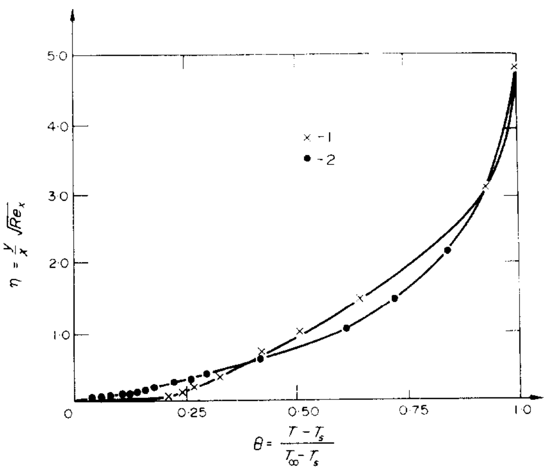

FIG. 4. Temperature distribution in the boundary layer with liquid evaporation from porous glass. 1, plate centre; 2, "dry" heat transfer.

To determine the conditions for the occurrence of the temperature jump a special experiment was made on evaporative cooling in the drying regime. It was found that the temperature jump value over the body surface decreased with time (Fig. 5).

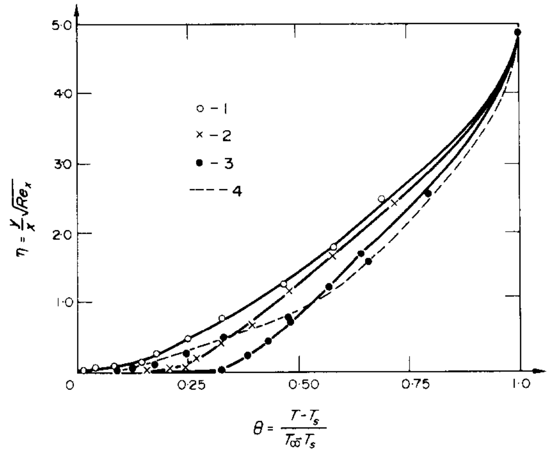

FIG. 5. Temperature distribution in the boundary layer with drying of moist porous glass. 1, $\tau = 0$; 2, $\tau = 3$ h; 3, $\tau = 7$ h; 4, "dry" heat transfer.

An analysis of temperature curves within the capillary-porous body and in the boundary layer allows us to make the following suppositions regarding the intense evaporative cooling mechanism and also the nature of the temperature jump and mass-transfer mechanism in the boundary layer over a surface of a porous body of poor heat conductivity. As in the case of a body with high thermal conductivity evaporation from glass spheres is of volume character but dimensions of the volume evaporation zone is considerably larger (Fig. 6). Under the influence of internal heat flux the temperature field over the body section is highly non-uniform because of poor thermal conductivity which creates favourable conditions for the occurrence of a pressure gradient within the body. The pressure gradient causes liquid dispersion, meniscus breakage in pores and carry-over of vapour–liquid mixture to the body surface.

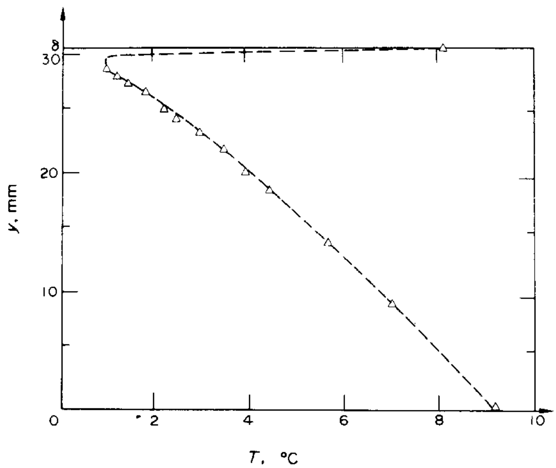

FIG. 6. Temperature distribution inside porous glass.

Owing to instability of liquid menisci the body volume appears to be permeable to air. Penetrating deep into the body air causes an intense volume evaporation of liquid which leads in its turn to an increase of the pressure gradient. A vapour pocket formed by liquid evaporation in the body depth, i.e. in a relatively heated region, on its way to the surface passes colder body sections and, on being enriched with cold vapour formed in these sections, appears to be close to supersaturation. Being carried out under a pressure gradient influence the density of the vapour–gas–liquid mixture consisting of supersaturated cold vapour, cold air and water droplets turns out to be higher than that of the surrounding medium. As a result, while moving out of the porous body the mixture is subjected to gravitational force directed against the motion. At definite thermodynamic conditions there occurs dynamic equilibrium of inertia forces acting on the mixture, and of diffusion and convection transfer, and the mixture as if "hangs" in a condensing state. Under the action of these factors, namely supersaturation state, presence of condensation centres in the form of liquid droplets and action of the mass force field, vapour condensation proceeds causing a jump-like temperature change near the body surface that has been observed in the experiments.

An analogous scheme of the evaporation

mechanism and temperature jump nature finds verification in experimental results on liquid evaporation conducted in the drying regime. As was remarked above the temperature jump in the surface layer decreased down to zero with a decrease of the body moisture content. This may be easily explained by considering the character of the change of the interrelation between moisture and porous body material with decrease in the moisture content. At the onset of the experiment the volume evaporation zone was saturated with capillary-bound moisture providing high evaporation rate and being readily dispersed. In this period the process proceeded according to the scheme described above, being characterized by carry-over of liquid droplets, vapour condensation and considerable temperature jump near the body surface (Fig. 5, curve 1). As evaporation proceeds, capillary moisture in the body decreases and a portion of adsorption-bound moisture increases. The adsorption-bound moisture is absolutely not ready for dispersion and is characterized by retarded evaporation rate. As a result, carry-over of moisture and vapour condensation connected with it are reduced and this produces a decrease in temperature jump (Fig. 5, curve 2).

At a definite value of moisture content the capillary moisture is completely absent in the upper body part. Renewal of the adsorption moisture evaporated by means of capillary vapour condensation proceeds slowly and gradually the surface zone of the body increases in temperature. Occurring in the body depth the capillary moisture evaporation cannot provide carry-over transfer of liquid droplets through semi-dry body thickness: besides, vapour passing through the surface zone succeeds in being heated. As a result there are no conditions present for vapour condensation and the temperature jump disappears (Fig. 5, curve 3).

The phenomena stated (filtration carry-over of liquid coolant and condensation heat release in the boundary layer), which adversely affect the efficiency characteristics of evaporative cooling, appear only in the presence of a considerable inner heat release. This verifies experimentally the considerations made above on uselessness of materials with poor thermal conductivity for protection in the case of inner heat load.

It follows from the experimental results that a real evaporative cooling process under vacuum conditions differs considerably from the process usually treated in theoretical analysis, the degree of difference depending on the thermal conductivity coefficient λ_b of the capillary-porous material and on the presence of internal heat flux q_{int}. The influence of these parameters is of qualitative nature and leads to the following peculiarities:

(1) liquid evaporation within a body proceeds not in a plane but is of a pronounced volume character;

(2) developing within a body the overall pressure gradient is caused not only by convection–diffusion vapour transfer but by volume evaporation which is of non-isothermal character due to the internal heat flux;

(3) under a pressure gradient action vapour is transferred into an external boundary layer as part of a vapour–gas–liquid mixture which contributes to the occurrence of secondary phase transformations inside the boundary layer.

The established peculiarities of evaporative cooling lead to the conclusion that, under conditions of rarefaction and simultaneously acting external and internal heat fluxes, the process realization on the basis of complex application of materials with poor and good thermal conductivity appears to be most rational. A porous heat-protection wall should include an inner section made of material with good thermal conductivity and an outer, thinner, section made from heat-insulation material which is hydrophobic with respect to liquid coolant. The latter circumstance is of importance since it provides the optimum distribution of evaporation front inside a wall. Liquid will evaporate mainly at the interface of the two sections and only partly inside the hydrophobic heat insulator thus moderating temperature distribution over the section. Such a thermal protection system is universal regarding any heat flux and possesses properties of an unique diode which without any hindrance allows an internal heat flux pass to the evaporation zone and prevents an external heat flux to penetrate into the body.

REFERENCES

1. E. R. G. Eckert and R. M. Drake, Jr., *Heat and Mass Transfer*. McGraw-Hill, New York (1959).
2. A. V. Luikov, *Theory of Drying*. Energiya, Moscow (1968).
3. A. V. Luikov and G. V. Vasilieva, Study of heat and mass transfer in liquid evaporation from a capillary-porous body, *Inzh-Fiz. Zh.* **14** (3), 395 (1968).
4. D. F. Dyer, Bulk and diffusional transport of gases at non-uniform pressure, *Trans. Faraday Soc.* **63** (3) (1967).
5. P. P. Morgan and S. Yerazunis, Heat and mass transfer between an evaporative interface in a porous medium and an external gas stream, *A.I.Ch.E. Jl.* 132 (1967).

PARTICULARITES DU REFROIDISSEMENT PAR EVAPORATION DANS UN GAZ RAREFIE

Résumé— Le processus de refroidissement par évaporation de corps poreux est considéré sous des conditions de raréfaction et de flux thermiques internes.

Basées sur une analyse théorique et sur une étude expérimentale, des relations importantes ont été établies et des conditions optimales de refroidissement par évaporation ont été obtenues. On montre que le mécanisme d'évaporation d'un refroidissement par liquide sous vide est contrôlé par les propriétés thermophysiques et structurales du corps poreux et de la récession de la zone d'évaporation.

BESONDERHEITEN DER VERDUNSTUNGSKÜHLUNG IN VERDÜNNTEN GASEN

Zusammenfassung— Verdunstungskühlung an porösen Körpern wird untersucht bei Vakuum und innerer Wärmeerzeugung.

Auf Grund einer theoretischen Analyse und einer experimentellen Untersuchung werden die Hauptbeziehungen aufgestellt und die optimalen Bedingungen für die Verdunstungskühlung gewonnen.

Es hat sich gezeigt, dass der Verdunstungsmechanismus der Flüssigkeitskühlung unter Vakuum durch die thermophysikalischen und Struktureigenschaften des porösen Körpers und das Zurückweichen der Verdunstungszone bestimmt wird.

ОСОБЕННОСТИ ИСПАРИТЕЛЬНОГО ОХЛАЖДЕНИЯ В РАЗРЕЖЕННОМ ГАЗЕ

Аннотация—Рассматривается процесс испарительного охлаждения пористых тел в условиях разрежения и совместного действия внешней и внутренней тепловых нагрузок.

На основе теоретического анализа и экспериментального исследования установлены основные связи и выявлены оптимальные условия проведения испарительного охлаждения. Показано, что механизм испарения жидкого охладителя в вакууму определяется теплофизическими и структурными характеристиками пористого тела и величиной заглубления зоны испарения.